ISSN 1062-8738, Bulletin of the Russian Academy of Sciences: Physics, 2008, Vol. 72, No. 5, pp. 664–669. © Allerton Press, Inc., 2008.
Original Russian Text © A.E. Afanas'ev, P.N. Melent'ev, V.I. Balykin, 2008, published in Izvestiya Rossiiskoi Akademii Nauk. Seriya Fizicheskaya, 2008, Vol. 72, No. 5, pp. 701–706.

Atomic Surface Trap Based on Quantum Adsorption

A. E. Afanas'ev, P. N. Melent'ev, and V. I. Balykin

Institute of Spectroscopy, Russian Academy of Sciences, Troitsk, Moscow oblast, 142190 Russia
e-mail: afanasiev@isan.troitsk.ru

Abstract—A method of quantum adsorption of atoms on a surface has been proposed and experimentally implemented. Loading of atoms into a surface potential well (adsorption) was realized due to the loss of kinetic energy upon inelastic collision of two laser-excited atoms. This scheme was realized for Rb atoms adsorbed on the surface of a YAG crystal. The dependence of the quantum adsorption rate on the laser frequency has been investigated. A possibility of fabricating microstructures of arbitrary shape from atoms adsorbed on a dielectric surface is demonstrated and possibilities of producing nanostructures is discussed.

DOI: 10.3103/S1062873808050213

INTRODUCTION

Localization of neutral atoms [1–3] is important from both fundamental and applied points of view. To date, atomic traps based on the use of magnetic [4], electric [5], laser [3], and laser-magnetic (magneto-optical traps) [6] fields have been implemented. A characteristic feature of all these atomic traps is their small depth: about 10^{-2} K for magnetic and as high as 1 K for electric and magneto-optical traps; therefore, localization of atoms in such traps became possible only after development of methods of laser cooling of neutral atoms [7–9].

At the same time, it is well known that surface potential wells based on van der Waals forces or (and) chemical forces have a depth of about 10^1–10^3 K and; hence, can hold neutral atoms with fairly high kinetic energies (for example, spontaneous adsorption of atoms on a surface from the gas phase). Despite the evident advantages of atomic localization in a surface potential both from the fundamental (quantum-mechanical modification of spontaneous emission rate, Casimir effect) and practical (application in quantum informatics [10–12] and atomic chips [13]) points of view, such traps have not been implemented until now (we exclude the natural process of capture of an atom during its adsorption on a surface). The main problem is fabrication of a surface trap is the absence of effective methods for loading atoms into a surface well. In [14], a scheme of loading atoms into surface traps, which is based on photoassociation, was proposed for the first time. Photoassociation is the formation of a molecule from atoms upon absorption of a photon at the instant of their collision. Such light-induced "pairing" of atoms became possible after development of methods for laser cooling of atoms, which made it possible to significantly increase the phase density of atomic ensembles [15] (the probability of an atom–atom–photon ternary collision is proportional to the phase atomic density $\rho\lambda_B^3$, where ρ is the atomic density and λ_B is the de Broglie wavelength). Photoassociation probability can be also increased if one of the partners in a ternary collision has a macroscopic size. Such a situation arises upon collision of an atom with a solid surface exposed to laser radiation. In this case, the photoassociation rate for an atom on a surface can exceed the corresponding atom–atom photoassociation rate by many orders of magnitude (in the relation $S/\lambda_B^2 \gg 1$, where S is the surface area exposed to light). Nevertheless, loading of atoms into a surface trap with the use of photoassociation can be implemented only for ultracold atoms, and theoretical estimates show that the efficiency of this process is low even for ultracold atoms [14]. In [16], a wide spectrum of a Cs absorption line near a nanowaveguide was observed; this effect was assigned to transitions from the bound state of an atom in the van der Waals potential.

In this study, we propose a technique of fabricating a surface trap on the basis of a new mechanism of loading atoms into a surface trap and demonstrate implementation of such a trap by the example of neutral Rb atoms. We also consider fabrication of microstructures of an arbitrary shape from atoms localized on an insulator surface and point out the possibility of forming atomic nanostructures on a surface.

BASIC CONCEPT

The proposed mechanism of loading atoms into a surface trap is based on the effect of energy transfer to highly excited levels upon collision (energy-pooling collision), which is in inelastic collision of two excited atoms with subsequent transition of one of them to the ground state and transition of the other to a highly excited state [17–19]. The internal-energy defect is compensated for by the kinetic energy of the atoms. If

an atomic collision occurs in a potential surface well, an atom can be localized in this well.

Figure 1a shows the energy diagram of lower levels of an Rb atom. The $5^2P_{3/2}$ level of an Rb atom is populated upon absorption of 780-nm laser light. The $5d$ level has an energy close to the $5p + 5p$ asymptote for an Rb_2 molecule; therefore, it can be populated upon collision of excited atoms as a result of the energy-transfer to highly excited levels:

$$\text{Rb}\,(5p) + \text{Rb}\,(5p) + \Delta E \rightarrow \text{Rb}\,(5d) + \text{Rb}\,(5s). \quad (1)$$

Here, ΔE = 93 K is the difference between the total kinetic energy difference before and after the atomic collision (energy defect). As a result of a collision of two atoms (1), one of them relaxes to the ground state, and the other passes to the highly excited state $5d$. The energy defect is compensated for due to the translatory motion of the atoms; i.e., in the process (1), the kinetic energy of two atoms decreases by 93 K after the collision. The collisional energy transfer can easily be observed in the form of blue fluorescence, which is due to the transition of the atom from the $5d$ state to the $6p$ state, from which the atom relaxes to the ground state, emitting 420.2- and 421.6-nm photons [17–19]. If the collision of two excited atoms occurs near the bottom of a surface potential well, the kinetic-energy loss upon collision may lead to the localization of an atom in the surface potential (i.e., its adsorption), as schematically shown in Fig. 1b.

In this study, we investigated the quantum adsorption of an Rb atom near the surface of a YAG crystal. The atomic surface potential is considered as the sum of long-range attractive van der Waals potential and the short-range repulsive potential [20]

$$V(z) = V_0\exp[a\psi(R) - z], \quad (2)$$

where $\psi(R) = \psi(\mathbf{G}_0, x, y)$ is the function describing the surface relief, $\mathbf{G}_0$ is the reciprocal surface lattice vector, and x and y are the coordinates in the surface plane.

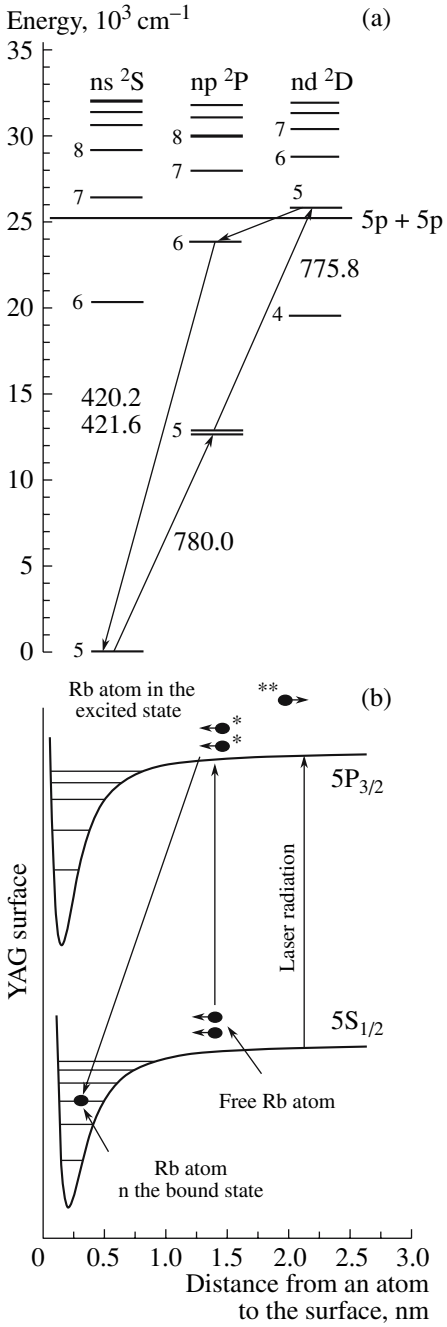

Fig. 1. (a) Energy diagram of the lower levels of an Rb atom. The $5d$ level has an energy close to that of the $5p + 5p$ asymptote for an Rb_2 molecule and, therefore, can be populated upon collision of excited atoms; (b) the kinetic-energy loss upon collision of two excited atoms near the bottom of the surface potential well may lead to localization of an atom in the surface potential.

EXPERIMENTAL

Quantum adsorption of Rb atoms was experimentally implemented using a sapphire cell filled with a vapor of Rb atoms. The cell windows are made of a YAG crystal. The cell temperature could be varied from room temperature to 240°C; the temperature of the cell windows exceeded that of the main part of the cell by 30°C. Under such cell heating conditions, the YAG windows are free of Rb atoms. Laser radiation was tuned to the resonance with the $5^2S_{1/2} - 5^2P_{3/2}$ transition, and the laser beam passed through the cell perpendicularly to the window plane. The laser beam size was varied from 0.5 to 2 mm, and the maximum laser power was 70 mW. The collisional energy transfer was observed in the form of blue luminescence of Rb atoms (λ = 420.2 and 421.6 nm) from the region exposed to the laser beam in the cell. The blue luminescence was detected through the monochromator using a photodiode.

The laser-induced adsorption of Rb atoms on the surface was accompanied by the formation of a thin surface atomic layer on the cell window at the place of

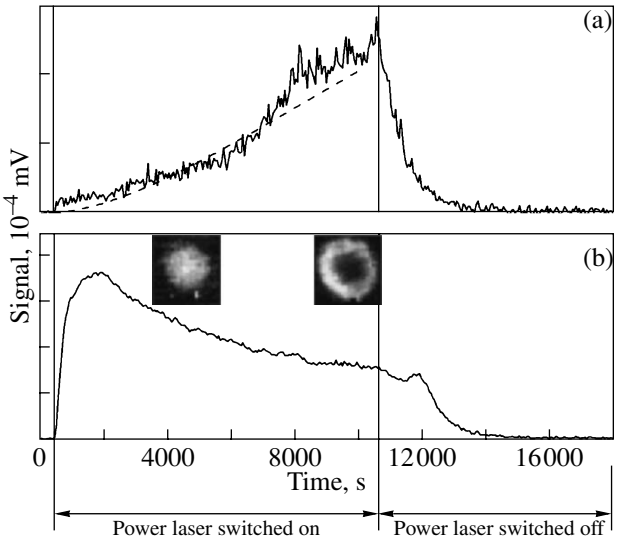

Fig. 2. Adsorption of atoms and subsequent growth of a monolayer on the surface as a function of the irradiation time of a cell with an Rb vapor in the slow (a) and fast (b) absorption modes (laser intensities $I = 150$ mW/cm^2 and 1.26 W/cm^2, respectively).

its intersection with the laser beam. Currently, two basic methods are used for diagnostics of the dynamics of adsorption of atoms on a surface: high-energy electron diffraction [21] and scanning tunnelling microscopy [22]. Since it was difficult to use both these methods in our experiment, we applied another approach to the diagnostics of atomic adsorption, which is based on scattering of incoherent light by the adsorbed atoms. A cell window with adsorbed atoms was illuminated by a parallel light beam from an incandescent lamp, and the radiation scattered by atoms was collected by a lens onto a CCD matrix. This scheme made it possible both to measure the total scattering signal from atoms and to determine the shape and structure of the spot formed by the adsorbed atoms on the surface.

Atomic adsorption and subsequent growth of a monolayer on the surface includes several stages: (i) adsorption of individual atoms, (ii) diffusion of adsorbed atoms along the surface, (iii) formation of growth centers of atomic islands on the surface, (iv) growth of islands, (v) coalescence of islands, and (vi) formation of an atomic monolayer [23, 24]. The sensitivity of our method for detecting atoms on a surface from light scattering was sufficient to observe the effects of island growth and monolayer formation.

RESULTS

Figure 2 illustrates the atomic adsorption and subsequent growth of a monolayer on a surface as a function of the time of laser irradiation of a cell with Rb vapor: the total intensity of scattered light from the Rb atoms adsorbed on the surface is plotted along the vertical axis and the cell irradiation time is plotted along the horizontal axis. Figure 2a corresponds to the slow-adsorption mode; it shows the change in the number of adsorbed atoms at a relatively slow rate of capture of atoms into the surface potential. Such a mode was obtained with a low laser intensity: $I = 150$ mW cm^{-2}. The initial portion of the curve corresponds to the first four stages of monolayer growth: from adsorption of individual atoms to the island growth. When laser radiation is switched off at the instant $t = 10^4$ s, the signal begins to decay due to the thermal desorption of atoms from the surface with a characteristic (temperature-dependent) time $t_d = 10^3$ s.

Figure 2b corresponds to the mode of fast atomic adsorption, which was obtained by increasing the laser intensity to $I = 1.26$ W cm^{-2}. During the time interval $t_s = 2 \times 10^3$ s, the intensity of scattered light from adsorbed atoms reaches saturation. With further exposure of the cell with a Rb vapor to laser radiation, the scattered signal decreases due to the transition of atomic adsorption to the mode of island coalescence and formation of a monolayer, which does not scatter light but specularly reflects it.

The image of the spot of adsorbed Rb atoms on the surface consists of individual scattering points. The left inset in Fig. 2 shows a CCD image of the spot of adsorbed Rb atoms in the initial stage of adsorption. The spot is formed by individual scattering centers, with the maximum concentration of scattering centers at the center of the laser spot, where the radiation intensity is maximum and, correspondingly, the adsorption rate is also maximum. The right inset in Fig. 2 is an image of adsorbed atoms in the later stage of atomic adsorption and growth of a monolayer, where individual islands are overlapped and an atomic monolayer is formed at the spot; the latter circumstance leads (due to the decrease in light scattering) to the formation of a "hole" in the image.

To calculate the atomic adsorption, we used a simple model of rate equations, describing the adsorption in the initial stage, where the degree of surface coverage by atoms $\theta \ll 1$ [23, 24]:

$$\frac{d\rho}{dt} = F(1-\theta) - \frac{\rho}{\tau_e} - F\rho - 2\sigma_0\rho - \sigma_i N, \qquad (3.1)$$

$$\frac{dN}{dt} = F\rho + \sigma_0\rho, \qquad (3.2)$$

$$\frac{d\theta}{dt} = 2[F\rho + \sigma_0\rho] + \sigma_i N - \frac{\theta}{\tau_e^{\text{island}}}, \qquad (3.3)$$

$$\frac{dh}{dt} = h_0 F\theta - \frac{h}{\tau_e^{\text{island}}}, \qquad (3.4)$$

$$R = \left(\frac{\theta}{N}\right)^{1/2}. \qquad (3.5)$$

Here, ρ is the density of adsorbed atoms; N is the density of atomic islands; θ is the degree of surface coverage; R is the radius of islands; τ_e is the thermal desorption rate of atoms; τ_e^{island} is the thermal desorption rate of islands; σ_0 is the cross section of island formation upon collision of two adsorbed atoms; σ_I is the cross section of attachment of an atom to an existing island, h_0 is the characteristic thickness of an island, which is determined by adsorption of atoms on its surface; and F is the rate of loading of Rb atoms into a surface well, which is determined by the rate of energy transfer to highly excited levels upon collision [17–19]:

$$F = \frac{1}{2}Kn_{5p}^2\Delta R. \quad (4)$$

Here, K is the rate of a given process, n_{5p} is the density of Rb atoms in the excited $5p$ state, and ΔR is the characteristic size of the surface potential in the direction normal to the surface. The signal from adsorbed atoms was determined on the basis of the standard model of light scattering from small (in comparison with the wavelength) metal particles [25]. Within this model, the light scattering cross section is determined by the expression

$$d\sigma = \frac{\omega^4}{2c^4}V^2|\alpha|^2(1+\cos^2\vartheta)dO, \quad (5)$$

where ω is the light frequency, c is the speed of light, V is the particle volume, α is the particle polarizability, ϑ is the observation angle, and dO is a solid angle element. In velocity equations (3), relation (4) for the deposition rate of atoms on the surface and relation (5) for the cross section of light scattering from adsorbed atoms were used. In Fig. 2a, the adsorption rate of atoms, calculated on the basis of velocity equations, is shown by a dotted line. It can be seen that the calculated dependence is in good agreement with the experimental curve.

We also investigated the dependence of the efficiency of quantum adsorption on the laser frequency. Laser radiation was scanned through the $D2$ absorption line of Rb vapor in the range $\Delta\nu = 24$ GHz. The laser scanning mode was monitored by measuring the absorption spectrum of laser radiation in an auxiliary cell with a Rb vapor (Fig. 3a). Simultaneously, during such frequency scanning, we measured the dependence of the fluorescence of Rb vapor in the cell studied, which is due to the $6p - 5s$ transition at the wavelength $\lambda = 420$ nm (blue emission). This dependence is shown in Fig. 3b. A characteristic feature of the frequency dependence of blue emission is the decrease in the fluorescence intensity at resonant frequencies. Suppression of the fluorescence signal and, correspondingly, the efficiency of collisional energy transfer to highly excited levels is explained by the relaxation of atoms at the $5p$ level as a result of the collisions with the cell walls. It is known [26] that, at high atomic vapor concentrations, the penetration depth of laser radiation into the atomic vapor region depends strongly on the radiation frequency. At laser frequencies near the resonance, radiation penetrates only at a depth of about the light wavelength λ and relaxation of the excited state of atoms due to the wall collisions occurs during the characteristic time $t = \lambda/V \sim 1$ ns, which is an order of magnitude smaller than the time of spontaneous emission of a Rb atom (~28 ns). At large detunings, laser radiation penetrates at a large depth, forming in this case a much higher concentration of excited atoms near the cell window surface.

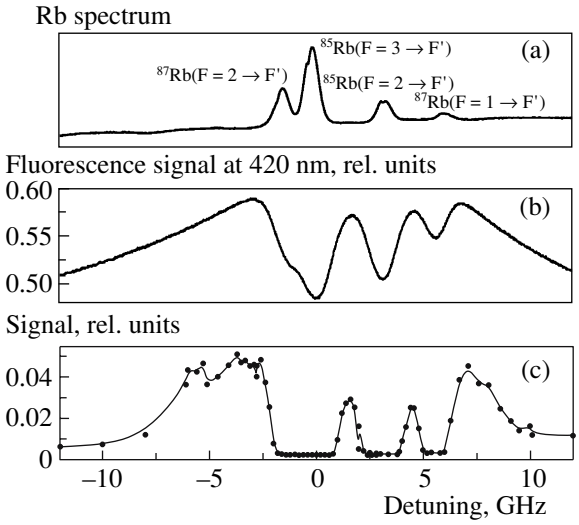

Fig. 3. (a) Absorption spectrum for a cell with an Rb vapor at room temperature; (b) the dependence of the Rb vapor fluorescence, which is due to the $6p - 5s$ transition at the wavelength $\lambda = 420$ nm (blue luminescence), on the laser frequency; and (c) light scattering signal from Rb atoms adsorbed on the surface as a function of the laser frequency (this signal characterizes the efficiency of loading atoms into the surface potential).

Figure 3c shows a signal of scattered light from Rb atoms adsorbed on the surface as a function of the laser frequency; this signal characterizes the efficiency of loading atoms into the surface potential. The measurement was performed at a cell temperature of 215°C. The cell temperature in this measurement was chosen from the requirement of fairly fast fabrication of an atomic structure on the surface (with a characteristic time of ~2 min) and, at the same time, sufficiently fast decay of the structure due to the thermal desorption after switching off the laser radiation (the characteristic lifetime of the structure was ~10 min). The measurement was performed as follows: (i) a fixed laser frequency was set; (ii) a spot of adsorbed Rb atoms was formed on the surface, and the number of adsorbed atoms was measured from the scattering signal; and (iii) laser radiation was switched off, and the atomic spot was destroyed due to the thermal desorption. Furthermore, the measurement was repeated at another laser frequency, etc. The dependence obtained is shown

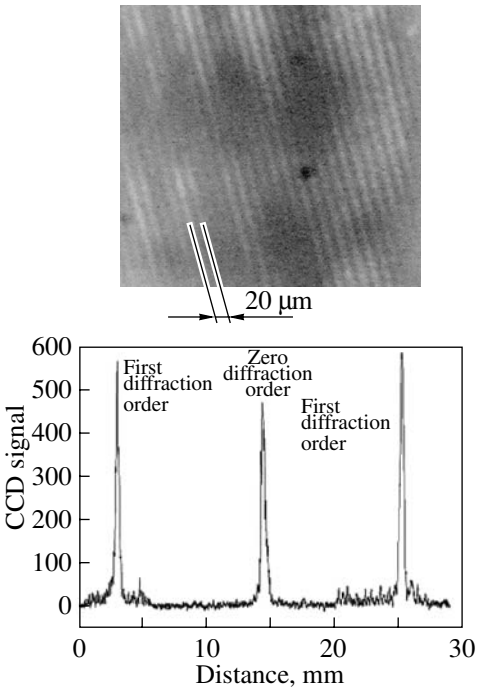

Fig. 4. Amplitude diffraction grating formed by Rb atoms adsorbed on a surface and the diffraction signal of probe laser radiation.

in Fig. 3c. Comparison of the spectral dependence of atomic adsorption (Fig. 3c) with the spectral dependence of the energy transfer to highly excited levels upon atomic collisions (Fig. 3b) shows identical behavior of both processes; this result proves that the energy-transfer effect is responsible for the loading of atoms into the surface potential well.

Quantum adsorption opens possibilities of creating atomic micro- and nanostructures of specified geometry on insulator surfaces. Figure 4 illustrates such a possibility by an example of fabrication of a grating of deposited Rb atoms on the cell window surface. To form such an atomic grating, the spatial profile of the laser beam was modulated by reflecting it from a Fresnel mirror. Illumination of the cell window by this spatially modulated laser beam formed an interference pattern of intensity maxima and minima on the window. Atoms were adsorbed in the regions of maximum intensity, while the regions of minimum intensity remained free of atoms. A regular system of bands of adsorbed atoms was formed in this way on the window surface. The grating period was 20 μm.

The array of atomic bands is an amplitude grating for the incident probe laser radiation. Therefore, a probe laser beam, being reflected from the developed atomic structure, undergoes diffraction. Figure 4 shows a CCD image of spatial intensity distribution for a probe laser beam reflected from a system of atomic bands on the cell window surface. The efficiency of the atomic diffraction grating is low; therefore, to provide simultaneous detection of three diffraction orders, the zero diffraction signal is decreased by a factor of 1500 using neutral filters. In Fig. 4, along with zero order, one can see first-order diffraction peaks.

Note that the use of laser radiation on the spatial nanoscale [27, 28] makes it possible to form atomic nanostructures of an arbitrary shape through quantum adsorption on a surface.

CONCLUSIONS

We have investigated the mechanism of laser-controlled quantum adsorption of Rb atoms on the surface of a YAG crystal on the basis of the effect of energy transfer to highly excited levels. A new type of a trap for neutral atoms is implemented, which is based on the surface potential well. Loading of atoms into a trap implies the effect of energy transfer upon collision of excited atoms. It is shown that atomic microstructures can be formed on surfaces with the use of surface traps. Application of laser nanofields opens possibilities for producing atomic nanostructures. It is shown that microstructures of arbitrary shape can be designed using quantum adsorption.

ACKNOWLEDGMENTS

This study was supported by the Russian Foundation for Basic Research, project nos. 06-02-16301-a, 06-08-01299-a, and 05-02-16370-a. We are grateful to V.G. Minogin and V.S. Letokhov for their helpful participation in the discussion of the results and to D. Sarkisyan's team for preparation of a cell with a Rb vapor.

REFERENCES

1. Adams, C.S. and Riis, E., *Prog. Quantum Electron.*, 1997, vol. 21, p. 1.
2. Balykin, V.I., Minogin, V.G., and Letokhov, V.S., *Rep. Prog. Phys.*, 2000, vol. 63, p. 1429.
3. Grimm, R., Weidemuller, M., and Ovchinnikov, Y., *Adv. At. Mol. Opt. Phys*, 2001, vol. 42, p. 95.
4. Migdall, A.L., Prodan, J.V., Phillips, W.D., et al., *Phys. Rev. Lett.*, 1985, vol. 54, p. 2596.
5. Wing, W.H., *Phys. Rev. Lett.*, 1980, vol. 45, p. 631.
6. Raab, E.L., Prentiss, M., Cable, A., et al., *Phys. Rev. Lett.*, 1987, vol. 59, p. 2631.
7. Chu, S., *Rev. Mod. Phys.*, 1998, vol. 70, p. 685.
8. Cohen-Tannoudji, C.N., *Rev. Mod. Phys.*, 1998, vol. 70, p. 707.
9. Phillips, W.D., *Rev. Mod. Phys.,* 1998, vol. 70, p. 721.
10. Schlosser, N., Reymond, G., Protsenko, I., and Grangier, P., *Nature (London)*, 2001, vol. 411, p. 1024.
11. Kuhr, S., Alt, W., Schrader, D., et al., *Science,* 2001, vol. 293, p. 278.
12. Sackett, C.A., Kielpinski, D., King, B.E., et al., *Nature (London)*, 2000, vol. 404, p. 256.

13. Eriksson, S., Trupke, M., Powell, H.F., et al., *Eur. Phys. J. D*, 2005, vol. 35, p. 135.
14. Passerat de Silans, "., Farias, B., Oriá, M., Chevrollier, M., *Appl. Phys. B*, 2006, vol. 82, p. 367.
15. Mackie, M. and Javanainen, J., *Phys. Rev. A: At., Mol., Opt. Phys.*, 1999, vol. 60, p. 3174.
16. Nayak, K.P., Melentiev, P.N., Morinaga, M., et al., *Optics Express*, 2007, vol. 15, p. 5431.
17. Jabbour, Z.J., Namiotka, R.K., Huennekens, J., et al., *Phys. Rev. A: At., Mol., Opt. Phys.*, 1996, vol. 54, p. 1372.
18. Barbier, L. and Cheret, M., *J. Phys. B: At. Mol. Phys.,* 1983, vol. 16, p. 3213.
19. Ban, T., Aumiler D., Beuc R., Pichler G. *Eur. Phys. J. D.,* 2004, vol. 30, p. 57.
20. Vargas, M.C. and Mochau, W.L., *Surf. Sci.* 1998, vol. 409, p. 130.
21. *Reflection High-Energy Electron Diffraction and Reflection Imaging of Surfaces*, Larsen, P.K. and Dobson, P.J., Eds., NATO ASI Series B: Physics, vol. 188; New York: Plenum, 1987.
22. Stroscio, J.A., Pierce, D.T., and Dragoset, R.A., *Phys. Rev. Lett.*, 1993, vol. 70, p. 3615.
23. Jensen, P., *Rev. Mod. Phys.,* 1999, vol. 71, p. 1695.
24. Jensen, P., Larralde, H., and Pimpinelli, A., *Phys. Rev. B: Condens. Matter Mater. Phys.*, 1997, vol. 55, p. 2556.
25. Landau, L.D. and Lifshitz, E.M., *Electrodynamics of Continuous Media,* New York: Pergamon, 1975.
26. Bambini, A. and Geltman, S., *Phys. Rev. A: At., Mol., Opt. Phys.*, 1994, vol. 50, p. 5081.
27. Balykin, V.I., Klimov, V.V., and Letokhov, V.S., *Opt. Photonics News*, 2005, vol. 16, p. 33.
28. Balykin, V.I and Klimov, V.V, in *Handbook of Theoretical and Computational Nanotechnology*, Ricth, M. and Schommers, W., Eds., New York: ASP, 2006, vol. 7.